J. Phase Equilib. Diffus. (2018) 39:324–343
https://doi.org/10.1007/s11669-018-0633-4

Experimental Investigation and Thermodynamic Calculation of Phase Equilibria in the Mg-Pb-Sn Ternary System

Dong Wang[1,2,3] · Jianhua Zhu[3] · Shangheng Wang[3] · Hongtao Chen[1] · Xingjun Liu[1,4] · Cuiping Wang[1,4]

Submitted: 6 February 2018 / in revised form: 10 April 2018 / Published online: 7 May 2018

Abstract The phase equilibria of the Mg-Pb-Sn ternary system were investigated using a combined method of electron probe microanalyzer and x-ray diffraction. Three isothermal sections of the Mg-Pb-Sn ternary system at 200, 300 and 400 °C were experimentally established. The phase equilibria of Mg-Pb-Sn ternary system were thermodynamically assessed by using CALPHAD (Calculation of Phase Diagrams) method on the basis of the presently determined experimental data. A consistent set of thermodynamic parameters has been derived for describing the Gibbs free energies of each solution phase and intermetallic compound in the Mg-Pb-Sn ternary system. The calculated phase diagrams and thermodynamic properties in the Mg-Pb-Sn ternary system are in good agreement with experimental data.

Keywords microstructure · Mg-alloys · thermodynamic modeling · phase diagrams

✉ Dong Wang
wd6531742@163.com

[1] Department of Materials Science and Engineering, Shenzhen Graduate School, Harbin Institute of Technology, Shenzhen 518055, People's Republic of China

[2] Department of Materials Science and Engineering, College of Materials, Xiamen University, Xiamen 361005, People's Republic of China

[3] Research Center, Shenzhen Zhenhua Fu Electronics Co., Ltd, Shenzhen 518109, People's Republic of China

[4] Research Center of Materials Design and Applications, Xiamen University, Xiamen 361005, People's Republic of China

1 Introduction

Mg-based alloys are widely used as anode materials, such as in seawater activated battery, semi-fuel battery, secondary battery and air battery etc.[1–4] They possess many excellent properties such as high cell voltage, wide voltage range, high power density capability, rapid activation, low density and large current capacity.[5–7] In addition, magnesium alloys undergo corrosion reactions and self-discharge, resulting in the reduction of current efficiency.[8, 9] The alloying elements such as Hg, Pb, Ga Al, Zn, Sn and RE (RE stands for the rare earth element) are introduced to improve the electrochemical behaviors of Mg-based alloys.[10–12] The phase diagram of the Mg-Pb-Sn system was investigated by Vegesack[13] using a thermal analysis technique and some vertical sections were presented. There was no ternary compound in the Mg-Pb-Sn system. Pogodin[14] determined the solubility range of the (Mg) hcp solid solution at 440 °C by electrical resistivity and microhardness measurement. Moreover, the enthalpies of mixing of the Mg_2Pb-Sn and Mg_2Sn-Pb liquid systems were measured by Sommer.[15] Howell and Eckert[16] optimized the parameters of liquid phase in the Mg-Pb-Sn system, but no comprehensive thermodynamic modeling of this system was performed. Lukas[17] researched the Mg-Pb-Sn ternary system on the base of the previous literature data. Jung and Kim[18] thermodynamically modeled the ternary system using the Modified Quasichemical Model, while no ternary interaction parameters were used to describe the phases in the Mg-Pb-Sn system. At present, although there are some experimental data, the phase boundaries are uncertain at low temperatures. Lukas,[17] Jung and Kim[18] assessed Mg-Pb-Sn ternary system. However, there still exist some problems for the present thermodynamic modeling of the Mg-Pb-Sn system. The

thermodynamic parameters[17, 18] cannot be directly employed in our Mg alloy thermodynamic database due to the model incompatibility. Thus, the precise investigations of the phase equilibra are needful for both experiment and thermodynamical assessment in the Mg-Pb-Sn ternary system. The CALPHAD (Calculation of Phase Diagrams) technique, which has been recognized to be an important tool to significantly reduce time and cost during the development of materials, can effectively provide a clear guidance for the materials design.[19–21] In order to develop a thermodynamic database of Mg-based alloys, the thermodynamic assessment of the Mg-Pb-Sn system was carried out by means of the CALPHAD method.

Three binary systems of Mg-Pb, Mg-Sn and Pb-Sn constituting the Mg-Pb-Sn ternary system have been reviewed by the previous investigations,[22–24] as shown in Fig. 1. One intermediate phase in the Mg-Pb system is observed, namely Mg_2Pb. Two eutectic reactions, $L \leftrightarrow (Mg) + Mg_2Pb$, $L \leftrightarrow (Pb) + Mg_2Pb$ occur at 466.2 and 248.7 °C, respectively. There are four phases in the Mg-Sn binary system, named (Mg), (Pb), Liquid and Mg_2Sn. There are two eutectic reactions ($L \leftrightarrow (Mg) + Mg_2Sn$, $L \leftrightarrow (Sn) + Mg_2Sn$) in Mg-Sn binary system. The Pb-Sn binary system has two solid solution phases ((Pb) and (Sn)). The stable solid phases and their crystal structures in the all three binary systems are listed in Table 1.

The purpose of the present work is to experimentally determine the phase equilibria of the Mg-Pb-Sn system at 200, 300 and 400 °C by using electron probe microanalyzer (EPMA) and x-ray diffraction (XRD). Additionally, the thermodynamic assessment of the Mg-Pb-Sn ternary system is carried out by means of the CALPHAD method. The obtained results may provide some information for the practical applications of the Mg-Pb-Sn alloys.

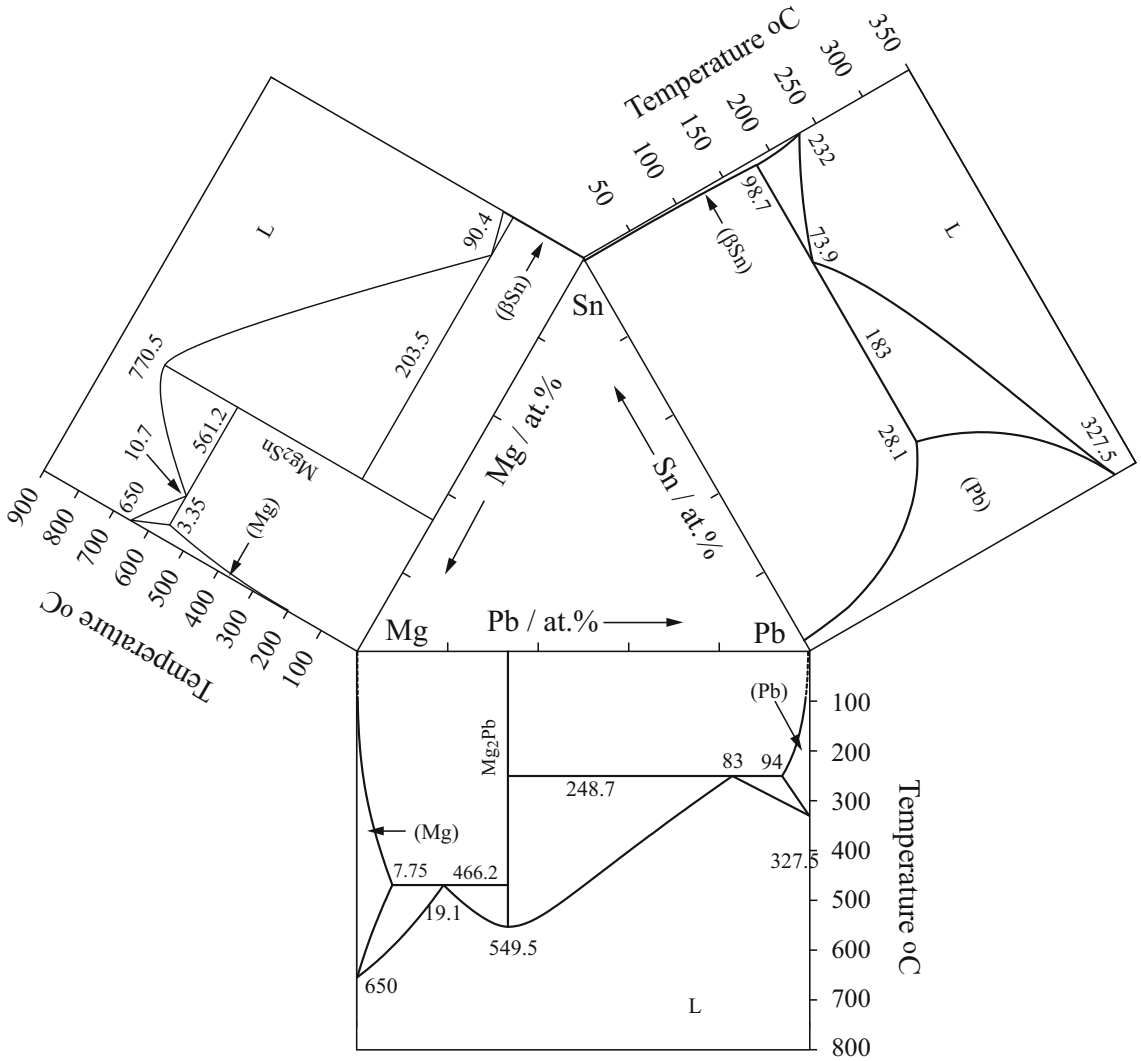

Fig. 1 Binary phase diagrams constituting the Mg-Pb-Sn ternary system[22–24]

Table 1 The structures and used model of phases in the Mg-Pb-Sn ternary system

Phase	Pearson's symbol	Prototye	Space Group	Struktur-bericht	Thermodyna-mic model	Used models
(Mg)	*hP*2	Mg	*P6*$_3$*/mmc*	*A*3	(Mg, Pb, Sn)	SSM
(Pb)	*cF*4	Cu	*Fm*-3 *m*	*A*1	(Mg, Pb, Sn)	SSM
(Sn)	*cF*4	βSn	*I4*$_1$-a*md*	*A*5	(Mg, Pb, Sn)	SSM
Mg_2Pb	*cF*12	CaF_2	*Fm*-3 *m*	*C*1	Mg_2(Pb, Sn)	SM
Mg_2Sn	*cF*12	CaF_2	*Fm*-3 *m*	*C*1	Mg_2(Sn, Pb)	SM

SSM subregular solution model, *SM* sublattice model

Table 2 Equilibrium compositions of the Mg-Pb-Sn ternary system determined in the present work

T (°C)	Alloy (at.%)	Annealed time (days)	Phase equilibria	Composition (at.%)					
			Phase 1/Phase 2/Phase 3	Phase 1		Phase 2		Phase 3	
				Pb	Sn	Pb	Sn	Pb	Sn
200	$Mg_{80}Pb_{10}Sn_{10}$	40	(Mg)/Mg_2Pb/Mg_2Sn	2.2	2.0	31.4	1.4	6.9	26.2
	$Mg_{60}Pb_{30}Sn_{10}$	40	Mg_2Pb/Mg_2Sn/(Pb)	31.7	1.5	7	26.3	96.3	1.7
	$Mg_{40}Pb_{40}Sn_{20}$	40	Mg_2Sn/(Pb)	3.3	29.5	87.8	9.9		
	$Mg_{50}Pb_{30}Sn_{20}$	40	Mg_2Sn/(Pb)	5.5	27.8	95.8	2.9		
	$Mg_{30}Pb_{30}Sn_{40}$	5	Mg_2Sn/(Pb)/Liquid	2.9	30.2	77.1	21.3	25.4	72.1
	$Mg_{40}Pb_{10}Sn_{50}$	5	Mg_2Sn/Liquid	1.9	30.9	21.6	74.8		
	$Mg_{40}Pb_5Sn_{55}$	5	Mg_2Sn/Liquid	1.3	31.7	9.1	84.4		
300	$Mg_{80}Pb_{10}Sn_{10}$	30	(Mg)/Mg_2Pb/Mg_2Sn	2.2	1.9	30.7	1.7	7.7	24.4
	$Mg_{60}Pb_{30}Sn_{10}$	2	Mg_2Pb/Mg_2Sn/Liquid	31.7	1.7	7.9	25.0	80.6	0.9
	$Mg_{40}Pb_{10}Sn_{50}$	2	Mg_2Sn/Liquid	0.9	31.5	18.9	68.5		
	$Mg_{40}Pb_{40}Sn_{20}$	2	Mg_2Sn/Liquid	1.7	30.8	84.6	10.2		
	$Mg_{30}Pb_{30}Sn_{40}$	2	Mg_2Sn/Liquid	1.3	31.3	41.5	50.8		
	$Mg_{40}Pb_{30}Sn_{30}$	2	Mg_2Sn/Liquid	2.1	30.8	72.4	22.8		
	$Mg_{50}Pb_{30}Sn_{20}$	2	Mg_2Sn/Liquid	2.1	30.3	86.5	3.5		
	$Mg_{35}Pb_{30}Sn_{35}$	2	Mg_2Sn/Liquid	1.3	31.3	55.5	38.7		
400	$Mg_{80}Pb_{10}Sn_{10}$	20	(Mg)/Mg_2Pb/Mg_2Sn	2.9	1.6	31.0	1.8	9.8	22.4
	$Mg_{60}Pb_{30}Sn_{10}$	1	Mg_2Pb/Mg_2Sn/Liquid	31.5	1.8	10.1	22.9	68.8	1.7
	$Mg_{40}Pb_{10}Sn_{50}$	1	Mg_2Sn/Liquid	1.0	32.3	12.2	63.2		
	$Mg_{40}Pb_{40}Sn_{20}$	1	Mg_2Sn/Liquid	3.2	29.5	77.5	11.1		
	$Mg_{30}Pb_{30}Sn_{40}$	1	Mg_2Sn/Liquid	1.3	32.7	31.6	50.2		
	$Mg_{40}Pb_{30}Sn_{30}$	1	Mg_2Sn/Liquid	2.3	30.9	64.7	23.2		
	$Mg_{50}Pb_{30}Sn_{20}$	1	Mg_2Sn/Liquid	3.7	28.5	78.5	4.3		
	$Mg_{35}Pb_{30}Sn_{35}$	1	Mg_2Sn/Liquid	1.7	31.6	44.8	37.9		

2 Experiment

2.1 Experimental Procedure

Magnesium (99.99 wt.%), Lead (99.99 wt.%) and Tin (99.99 wt.%) were used as starting materials. The samples each weighing about 20 g were prepared by melting in sealed tubes of Ta filled with high purity argon. The ingots were melted at least five times in order to achieve their homogeneity. The weight loss of each alloy during melting was generally less than 1.0% of the sample weight. Eight samples were prepared, and the compositions were listed in the Table 2. Afterwards, the ingots were cut into small pieces for heat treatment and further observation. All specimens were wrapped in Ta foil in order to prevent direct contact with the quartz ampoule, and put into quartz ampoule evacuated and backfilled with argon gas. The specimens were annealed at 200, 300 and 400 °C, respectively. The time of heat treatment varied from 1 to 40 days depending on the annealing temperature and the specimen

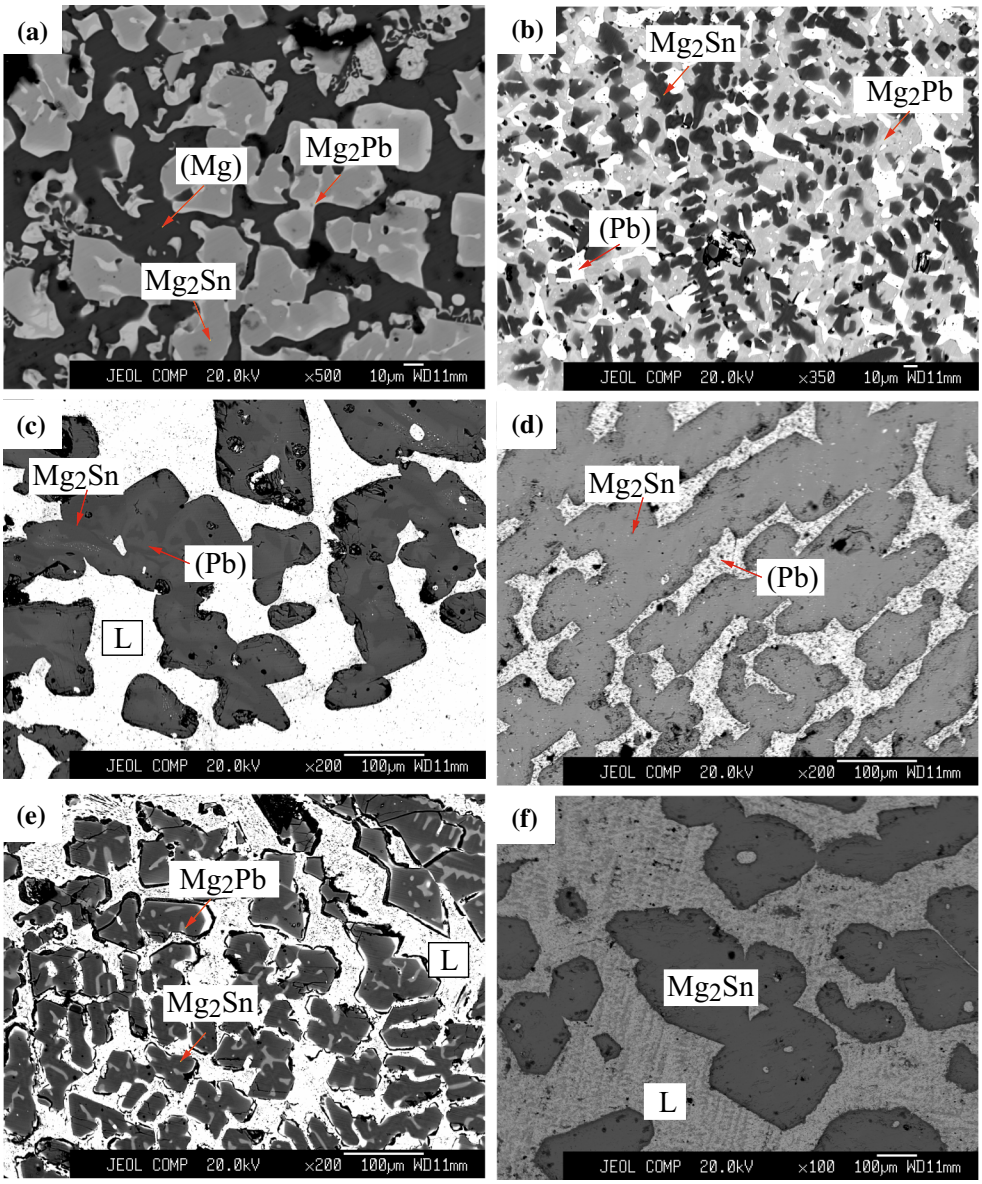

Fig. 2 Typical ternary BSE images of Mg-Pb-Sn ternary alloys obtained from: (a) the $Mg_{80}Pb_{10}Sn_{10}$ (at.%) alloy annealed at 200 °C for 40 days; (b) the $Mg_{60}Pb_{30}Sn_{10}$ (at.%) alloy annealed at 200 °C for 40 days; (c) the $Mg_{30}Pb_{30}Sn_{40}$ (at.%) alloy annealed at 200 °C for 5 days; (d) the $Mg_{40}Pb_{40}Sn_{20}$ (at.%) alloy annealed at 300 °C for 2 days; (e) the $Mg_{60}Pb_{30}Sn_{10}$ (at.%) alloy annealed at 300 °C for 2 days and (f) the $Mg_{40}Pb_{40}Sn_{20}$ (at.%) alloy annealed at 400 °C for 1 day

composition. After the heat treatment, the specimens were quenched into ice water.

After annealing procedure and standard metallographic preparation, the equilibrium compositions of the phases were measured by EPMA (JXA-8100R, JEOL, Japan). Pure elements were used as standards and the measurements were carried out at 20.0 kV. The x-ray diffraction (XRD) was used to identify the crystal structure of the constituent phases. The XRD measurement was carried out on a Phillips Panalytical X-pert diffractometer using Cu $K\alpha$ radiation at 40.0 kV and 30 mA. The data were collected in the range of 2θ from 20° to 90° at a step of 0.0167°.

2.2 Microstructure and Phase Equilibria

Phase identification is based on the equilibrium composition measured by EPMA and XRD results. The chemical composition is described using atomic ratio (at.%) in the present research. BSE images of typical Mg-Pb-Sn alloys are shown in Figs. 2(a)-(e). Figure 2(a) represents BSE image of sample $Mg_{80}Pb_{10}Sn_{10}$ annealed at 200 °C for 40 days, and the Mg_2Sn (Grey) phase and Mg_2Pb phase (offwhite) in the base of (Mg) phase (black). The microstructure of the $Mg_{60}Pb_{30}Sn_{10}$ alloy annealed at 200 °C for 40 days is shown in Fig. 2(b). It can be clearly

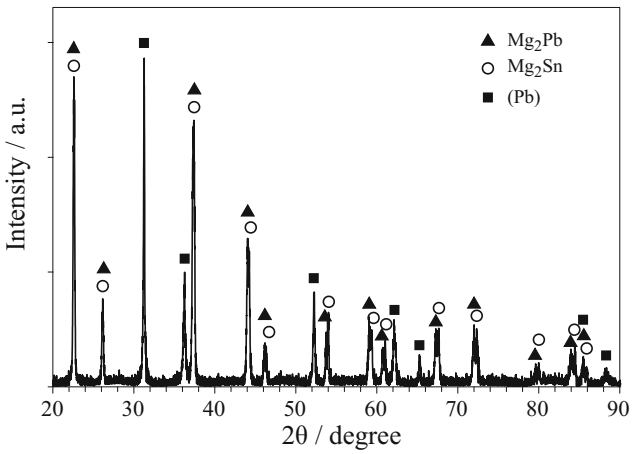

Fig. 3 X-ray diffraction patterns obtained of the $Mg_{60}Pb_{30}Sn_{10}$ (at.%) alloy annealed at 200 °C for 40 days

seen the presence of three phases ($Mg_2Pb + Mg_2Sn$ + (Pb)) for the $Mg_{60}Pb_{30}Sn_{10}$ alloy sample. Its XRD result is shown in Fig. 3(a), where the characteristic peaks of the Mg_2Pb, Mg_2Sn and (Pb) phases are confirmed. For $Mg_{60}Pb_{30}Sn_{10}$ alloy annealed at 200 °C for 5 days, as shown in Fig. 2(c), a three-phase microstructure of Mg_2Sn + (Pb) + Liquid is observed. Figure 2(d) presents the two-phase microstructure of Mg_2Sn + (Pb) for $Mg_{40}Pb_{40}Sn_{20}$ alloy annealed at 300 °C for 2 days. A two-phase equilibrium (Mg_2Sn + Liquid) is identified in the $Mg_{40}Pb_{40}Sn_{20}$ (at.%) alloy annealed at 400 °C for 1 day in Fig. 2(e), where the Mg_2Sn phase irregularly distributes in the liquid matrix. For $Mg_{40}Pb_{40}Sn_{20}$ alloy annealed at 400 °C for 1 day, a three-phase equilibrium of $Mg_2Pb + Mg_2Sn$ + Liquid is found, as shown in Fig. 2(e). All the equilibrium compositions of the Mg-Pb-Sn ternary system at 200, 300 and 400 °C are determined by EPMA and listed in Table 2.

3 Thermodynamic Assessment

The related information of stable solid phases and the models used in the Mg-Pb-Sn system are listed in Table 1.

3.1 Thermodynamic Models

3.1.1 Solution Phases

In the Mg-Pb-Sn ternary system, Gibbs free energies of the liquid, Fcc_A1, Hcp_A3 and Bct_A5 are described by the sub-regular solution model. According to this model, the molar Gibbs free energy of ϕ phase in the Mg-Pb-Sn ternary system is given by:

$$G_m^{\phi} = \sum_{i=Mg,Pb,Sn} {}^{0}G_i^{\phi} x_i + RT \sum_{i=Mg,Pb,Sn} x_i \ln x_i^{\phi} + {}^{ex}G^{\phi} \quad \text{(Eq 1)}$$

where G_i^{ϕ} is the Gibbs free energy of the pure component i in the respective reference state with the ϕ phase, and the term ${}^{ex}G^{\phi}$ is the excess free energy, which is expressed by the Redlich–Kister polynomials[25] as:

$$\begin{aligned} {}^{ex}G^{\phi} &= x_{Mg}x_{Pb}L^{\phi}_{Mg,Pb} + x_{Mg}x_{Sn}L^{\phi}_{Mg,Sn} + x_{Pb}x_{Sn}L^{\phi}_{Pb,Sn} \\ &\quad + x_{Mg}x_{Pb}x_{Sn}L^{\phi}_{Mg,Pb,Sn}, \\ L^{\phi}_{i,j} &= \sum_{m=0}^{n} {}^{m}L^{\phi}_{i,j}(x_i - x_j)^m, \\ L^{\phi}_{Mg,Pb,Sn} &= x_{Mg}\,{}^{0}L^{\phi}_{Mg,Pb,Sn} + x_{Pb}\,{}^{1}L^{\phi}_{Mg,Pb,Sn} + x_{Sn}\,{}^{2}L^{\phi}_{Mg,Pb,Sn} \end{aligned} \quad \text{(Eq 2)}$$

where $L^{\phi}_{i,j}$ is the interaction parameter in the i-j binary system, and the $L^{\phi}_{Mg,Pb,Sn}$ corresponds to the interaction parameters in the Mg-Pb-Sn ternary system. The coefficients of ${}^{n}L^{\phi}_{Mg,Pb,Sn}$ was evaluated in the present work.

3.1.2 The Intermetallic Compounds

No ternary intermediate phase is detected in the Mg-Pb-Sn ternary system in the present study. According to the experimental evidence and careful consideration, the thermodynamic models of the Mg_2Pb phase in the Mg-Pb binary system and Mg_2Sn phase in the Mg-Sn binary system are written as $(Mg)_2$: $(Pb)_1$ and $(Mg)_{2:}$ $(Sn)_1$, respectively, which are thought to be reasonable and accepted by the present work. The presently determined equilibrium compositions of the Mg_2Pb phase in the Mg-Pb-Sn ternary system clearly show that the Mg content almost keeps fixed. The above information suggests that Sn atoms substitute for Pb atoms in the Mg_2Pb phase. The intermetallic solution phase $Mg_2(Pb,Sn)_1$ is denoted in the TDB as "Mg_2X". Therefore, the Gibbs free energy of the $Mg_2(Pb,Sn)_1$ phase in the Mg-Pb-Sn ternary system is described as follows:

$$\begin{aligned} G_m^{Mg_2(Pb,Sn)} = & \sum_{\substack{i \\ (i=Pb,Sn)}} y_i^{I0} G_{Mg:i}^{Mg_2Pb} \\ & + RT\left(y_{Pb}^{I}\ln y_{Pb}^{I} + y_{Sn}^{I}\ln y_{Sn}^{I}\right) \\ & + y_{Pb}^{I}y_{Sn}^{I}\sum_{m=0}^{n} {}^{m}L_{Mg:Pb,Sn}\left(y_{Pb}^{I} - y_{Sn}^{I}\right)^m, \end{aligned} \quad \text{(Eq 3)}$$

where the ${}^{0}G_{Mg:i}^{Mg_2(Pb,Sn)}$ is the Gibbs free energy of the Mg_2Pb phase, when first one is occupied by the element Mg, the second sublattice is occupied by the element i ($i = Pb$ or Sn). The ${}^{m}L_{Mg:Pb,Sn}$ corresponds to the

Table 3 Optimized thermodynamic parameters in the Mg-Pb-Sn system

Parameters in each phase (J/mol)	References
Liquid phase, format $(Mg, Pb,Sn)_1$	
${}^0L^{Liq}_{Mg,Pb} = -33525 - 2.5T$	Ref. 26
${}^1L^{Liq}_{Mg,Pb} = -24600 + 9T$	
${}^2L^{Liq}_{Mg,Pb} = 2000 + 8T$	
${}^3L^{Liq}_{Mg,Pb} = 14500 - 3T$	
${}^0L^{Liq}_{Mg,Sn} = -30841.1+0.781T$	Ref. 27
${}^0L^{Liq}_{Mg,Mg_2Sn} = 5970.6 - 8.744T$	
${}^0L^{Liq}_{Mg_2Sn,Sn} = -12468.2 - 4.815T$	
${}^0L^{Liq}_{Pb,Sn} = 6204.5 - 0.67981T$	Ref. 28
${}^1L^{Liq}_{Pb,Sn} = 791.7 - 1.5219T$	
${}^0L^{Liq}_{Mg,Pb,Sn} = 80731.5+2.2T$	This work
${}^1L^{Liq}_{Mg,Pb,Sn} = 101463+5.23T$	
${}^2L^{Liq}_{Mg,Pb,Sn} = 19768.5 + 20T$	
Fcc phase, format $(Mg, Pb, Sn)_1$	
${}^0L^{Fcc}_{Mg,Pb} = -8657.34 - 10T$	Ref. 26
${}^0L^{Fcc}_{Pb,Sn} = 7145.3 - 2.30237T$	Ref. 28
${}^0L^{Fcc}_{Mg,Pb,Sn} = 105677.8 - 12T$	This work
${}^1L^{Fcc}_{Mg,Pb,Sn} = 141956.5 + 17T$	
${}^2L^{Fcc}_{Mg,Pb,Sn} = 75000+7.5T$	
Hcp phase, format $(Mg, Pb, Sn)_1$	
${}^0L^{Hcp}_{Mg,Pb} = -19187 - 9T$	Ref. 26
${}^1L^{Hcp}_{Mg,Pb} = -15587 + 15T$	
${}^0L^{Hcp}_{Mg,Sn} = -26256.5+6.234T$	Ref. 27
${}^1L^{Hcp}_{Mg,Sn} = -26256.5+6.234T$	
${}^0L^{Hcp}_{Pb,Sn} = 14000$	This work
${}^0L^{Hcp}_{Mg,Pb,Sn} = -47315 + 10T$	This work
${}^1L^{Hcp}_{Mg,Pb,Sn} = 45300 - 2T$	
${}^2L^{Hcp}_{Mg,Pb,Sn} = 32000+1.5T$	
$Mg_2(Pb, Sn)$ phase, format $(Mg)_2(Pb, Sn)_1$	
${}^0G^{Mg_2(Pb,Sn)}_{Mg:Pb} = -54206.85 + 17.8T + 2{}^0G^{Hcp}_{Mg} + {}^0G^{Fcc}_{Pb}$	Ref. 26
	Ref. 27
${}^0G^{Mg_2(Pb,Sn)}_{Mg:Sn} = -96165.9+339.999T - 66.285TLN(T) - 0.0121662T**2 + 96000T**(-1)+3.33828E-07T**3$	
${}^0G^{Mg_2(Pb,Sn)}_{Mg:Pb,Sn} = 5000+10.52T$	This work
${}^1G^{Mg_2(Pb,Sn)}_{Mg:Pb,Sn} = -5000 - 0.5T$	
Bct phase, format $(Pb, Sn)_1$	
${}^0G^{Bct}_{Pb,Sn} = 19700 - 15.89T$	Ref. 28

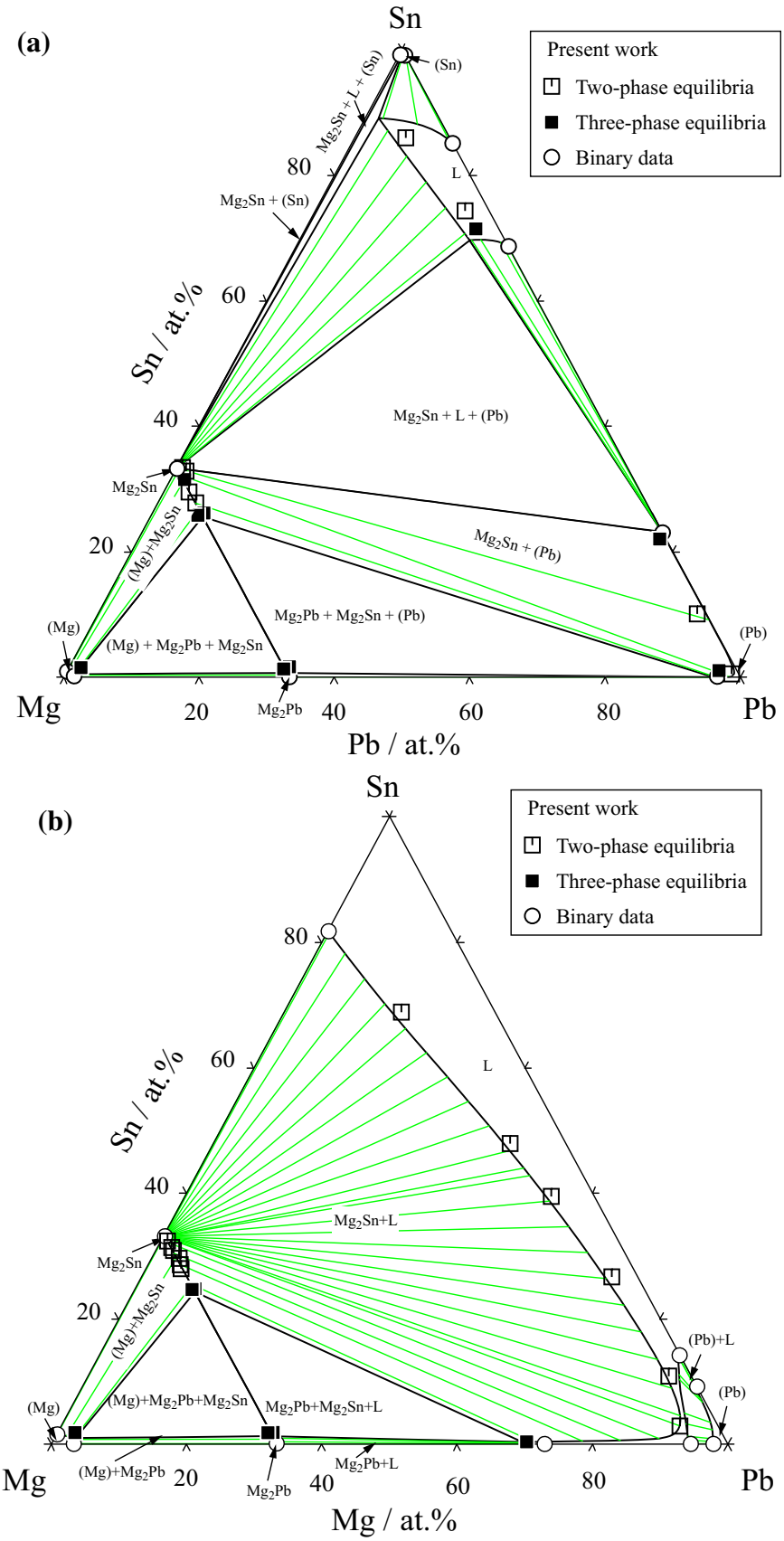

Fig. 4 Experimentally determined isothermal sections of the Mg-Pb-Sn system at: (a) 200 °C, (b) 300 °C and (c) 400 °C

Fig. 4 continued

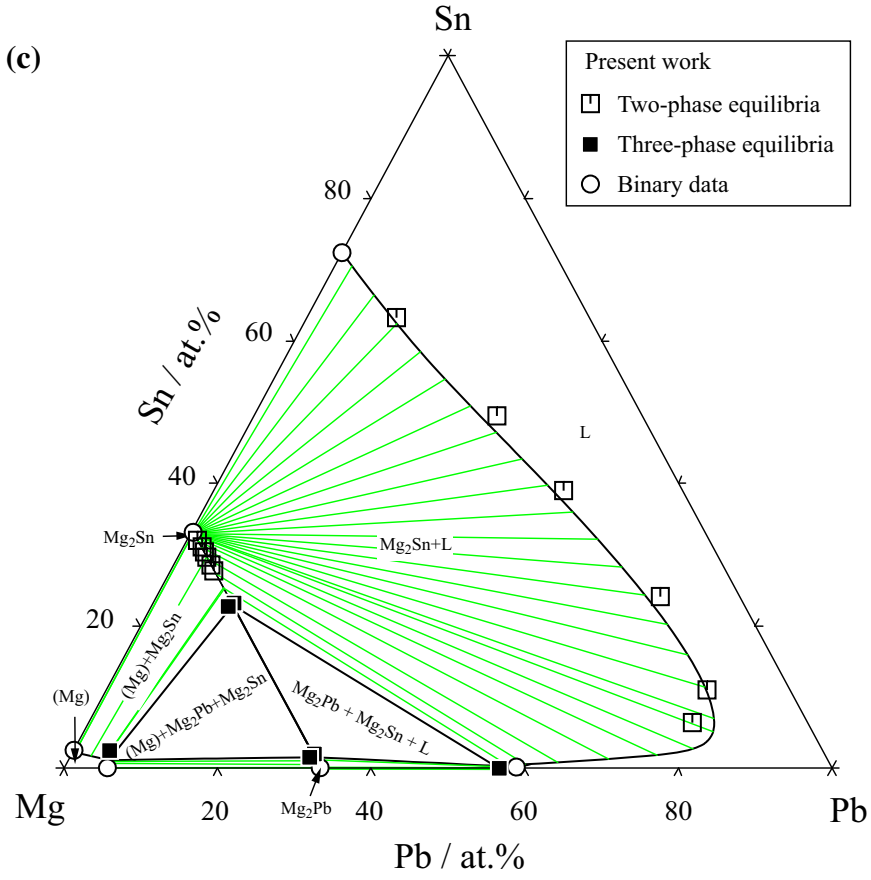

Fig. 5 The calculated vertical section at 10 at.% Sn in the Mg-Pb-Sn system compared with present experimental data

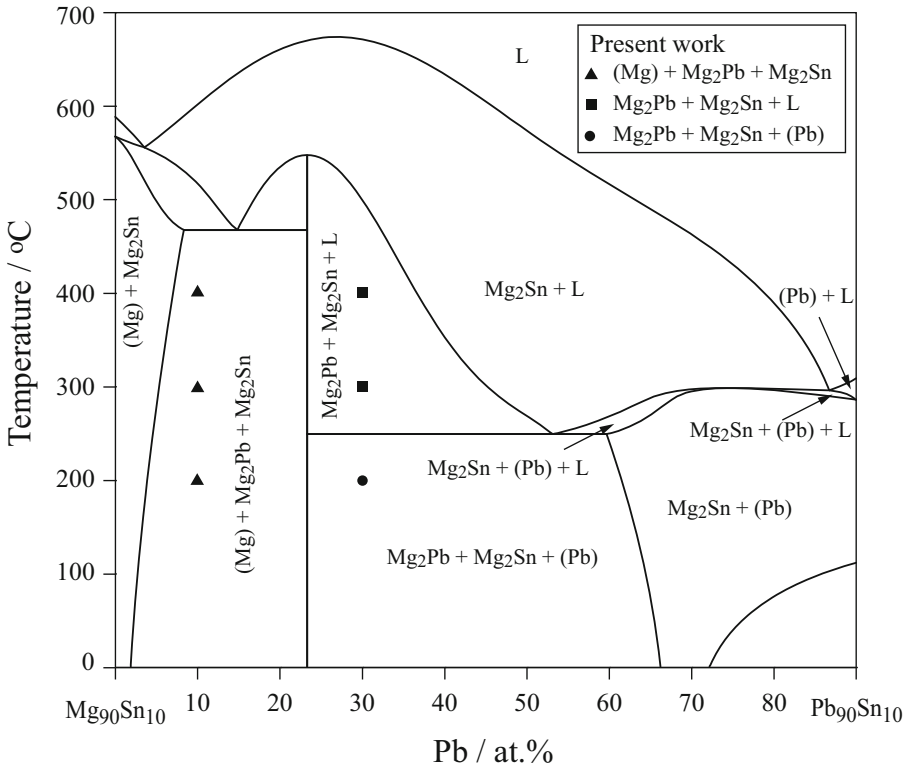

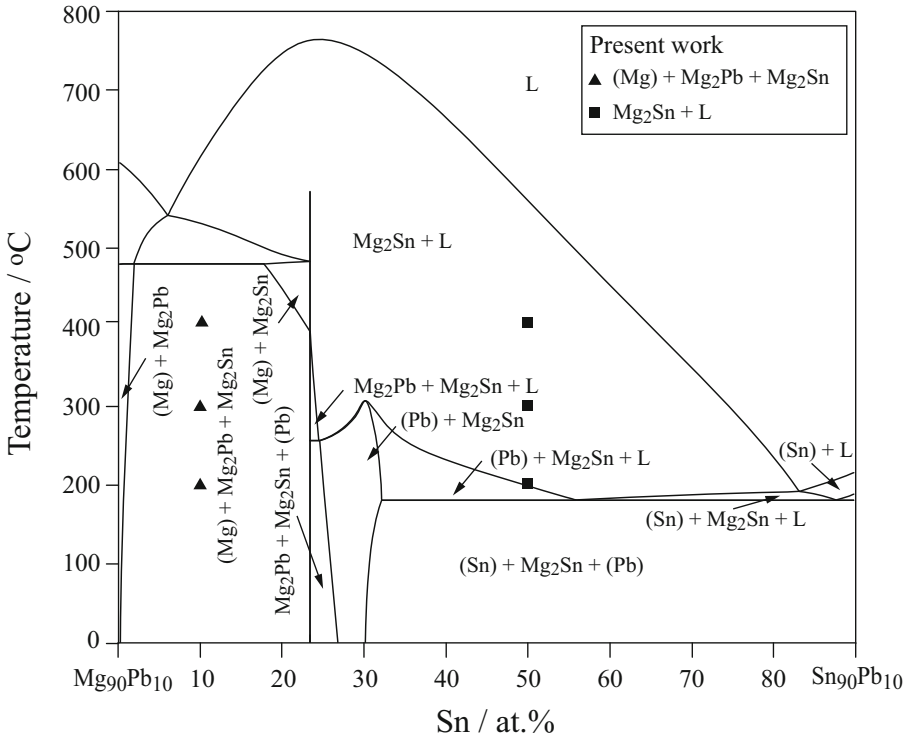

Fig. 6 The calculated vertical section at 10 at.% Pb in the Mg-Pb-Sn system compared with present experimental data

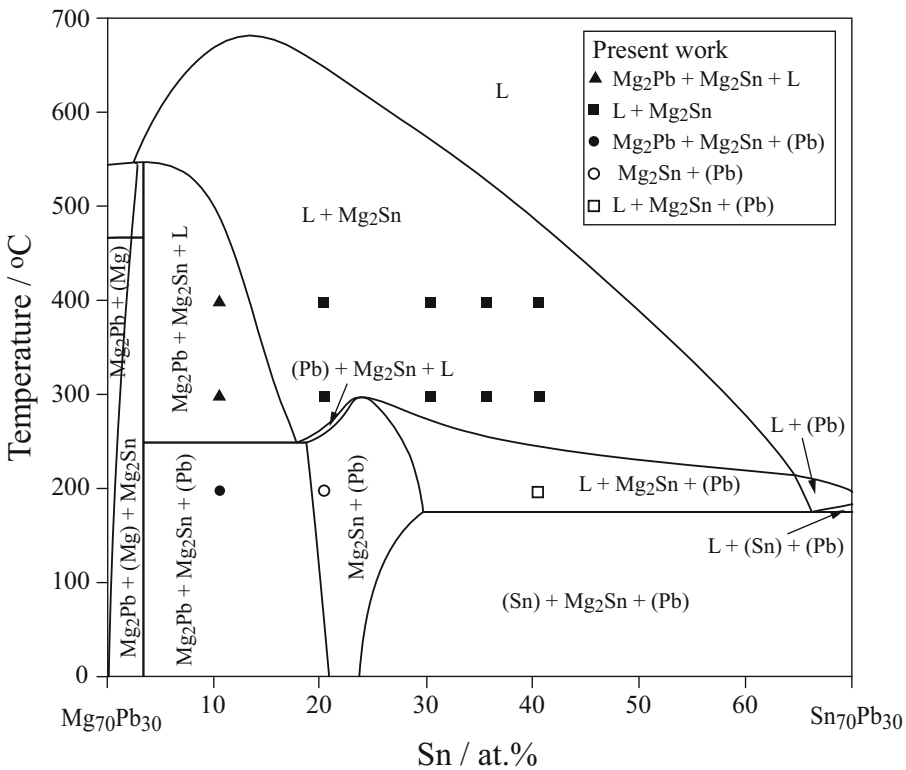

Fig. 7 The calculated vertical section at 30 at.% Pb in the Mg-Pb-Sn system compared with present experimental data

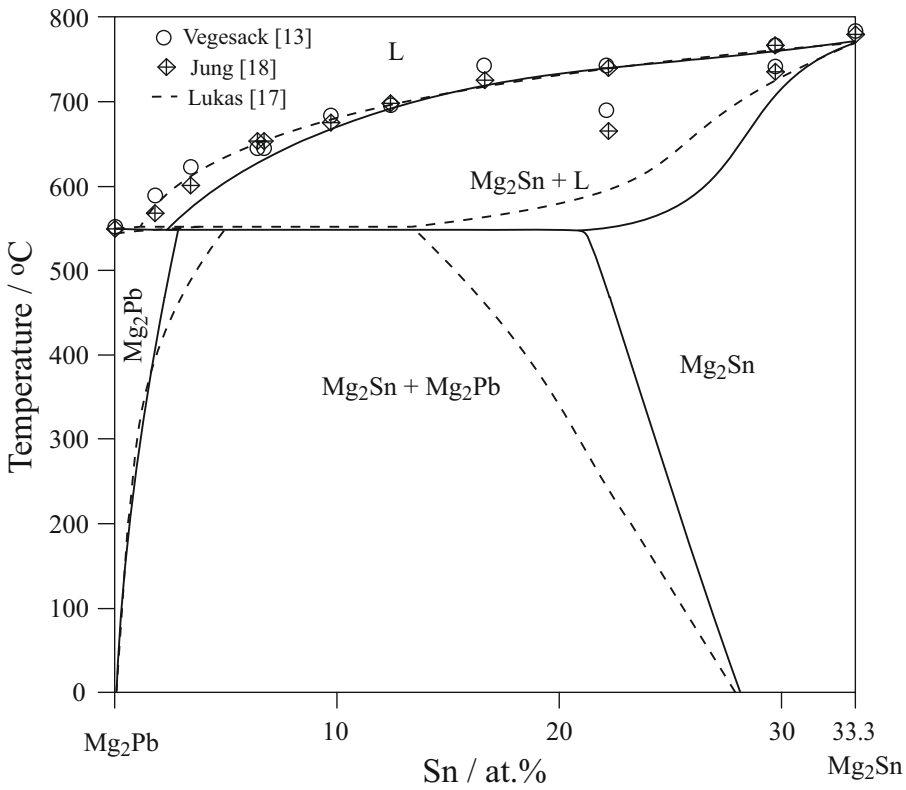

Fig. 8 The calculated vertical section of the Mg_2Sn-Mg_2Pb section in the Mg-Pb-Sn system compared with experimental data of Vegesack[13, 17, 18]

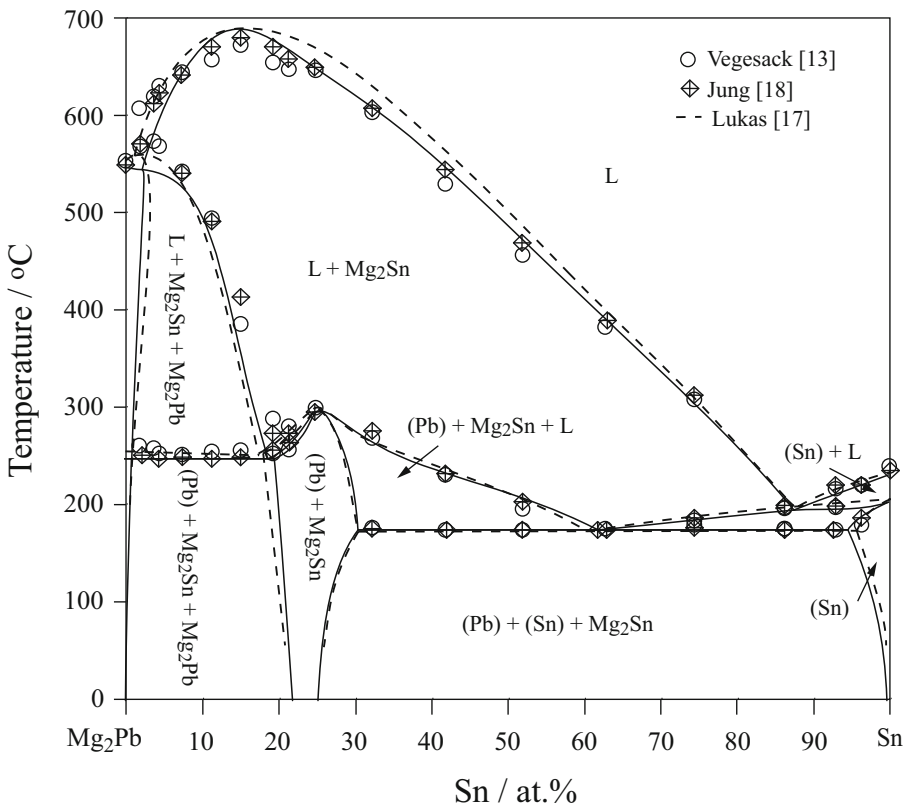

Fig. 9 The calculated vertical section of the Mg_2Pb-Sn section in the Mg-Pb-Sn system compared with experimental data of Vegesack[13, 17, 18]

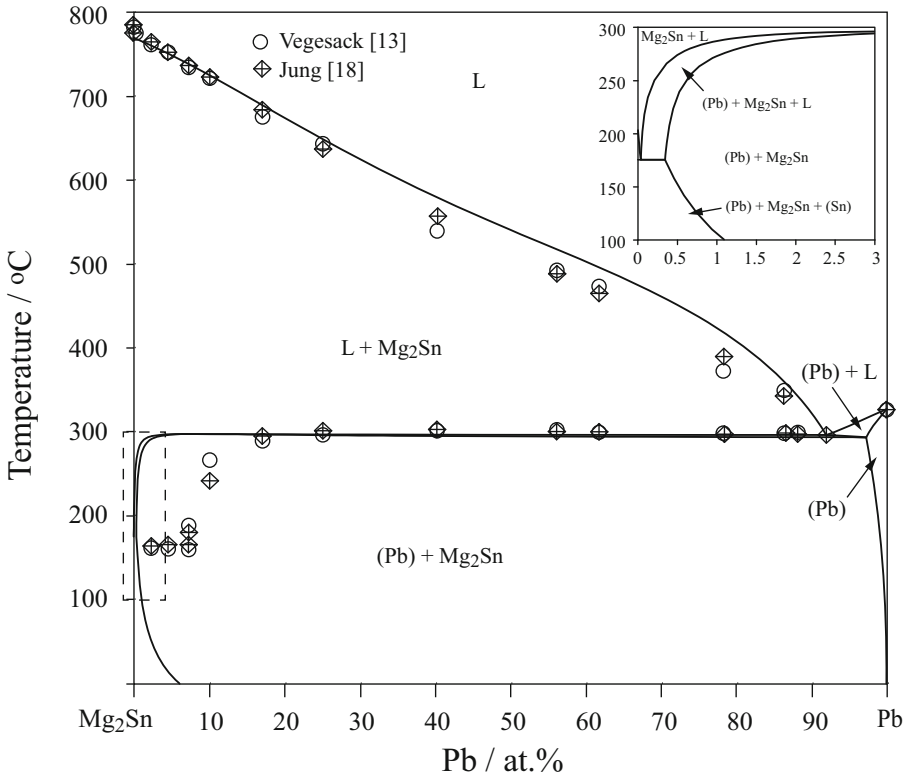

Fig. 10 The calculated vertical section of the Mg_2Sn-Pb section in the Mg-Pb-Sn system compared with experimental data of Vegesack[13, 18]

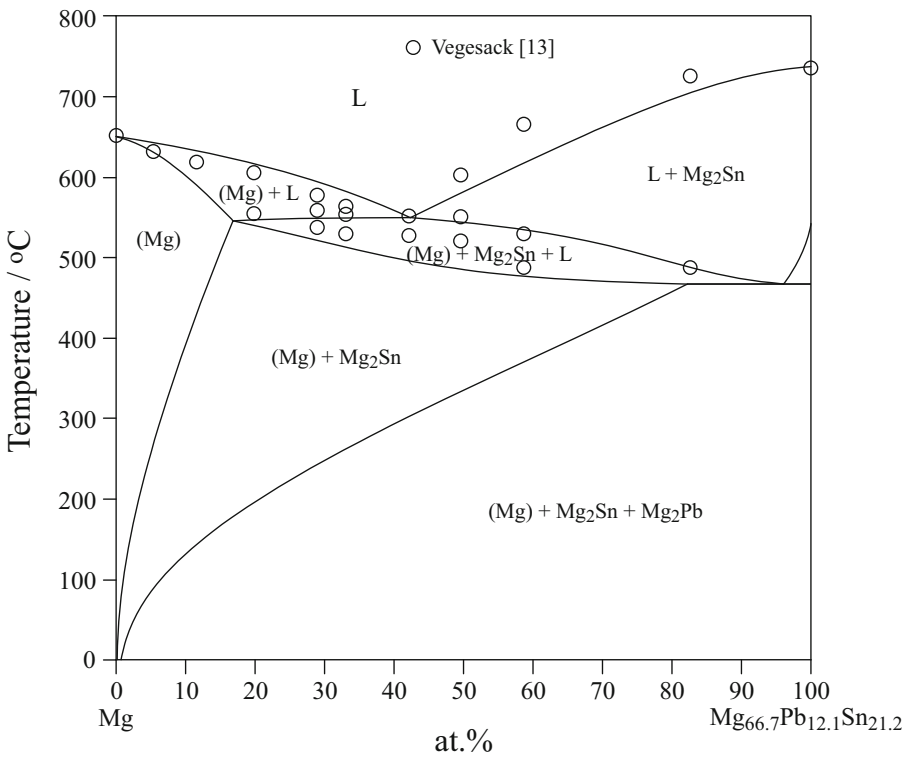

Fig. 11 The calculated vertical section of the Mg-$Mg_{66.7}Pb_{12.1}Sn_{21.2}$ section in the Mg-Pb-Sn system compared with experimental data of Vegesack[13]

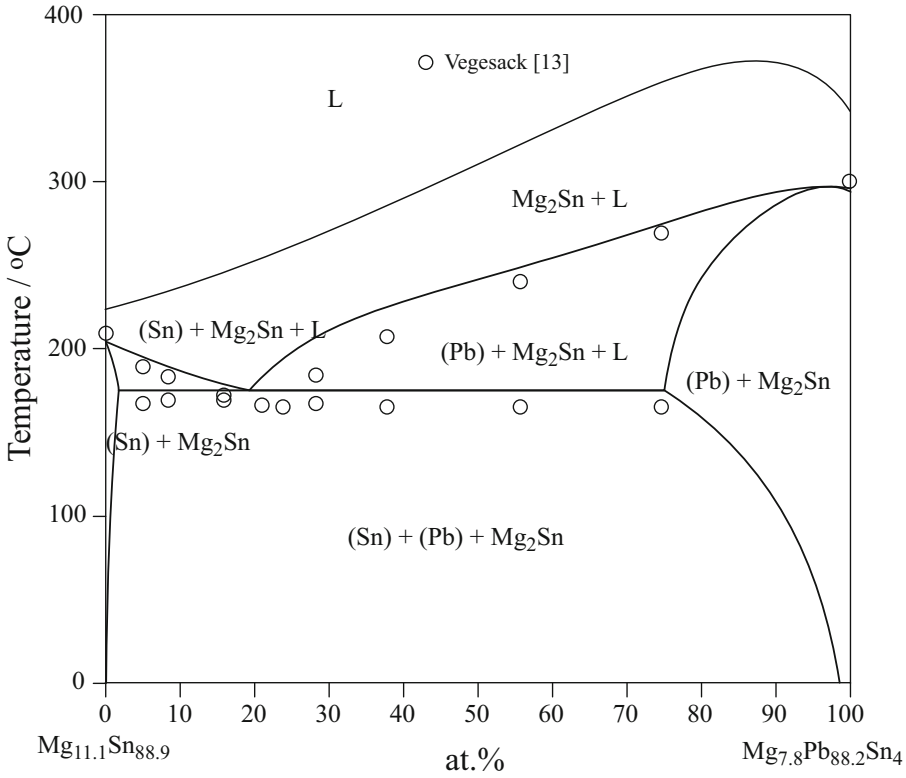

Fig. 12 The calculated vertical section of the $Mg_{11.1}Sn_{88.9}$-$Mg_{7.8}Pb_{88.2}Sn_4$ section in the Mg-Pb-Sn system compared with experimental data of Vegesack[13]

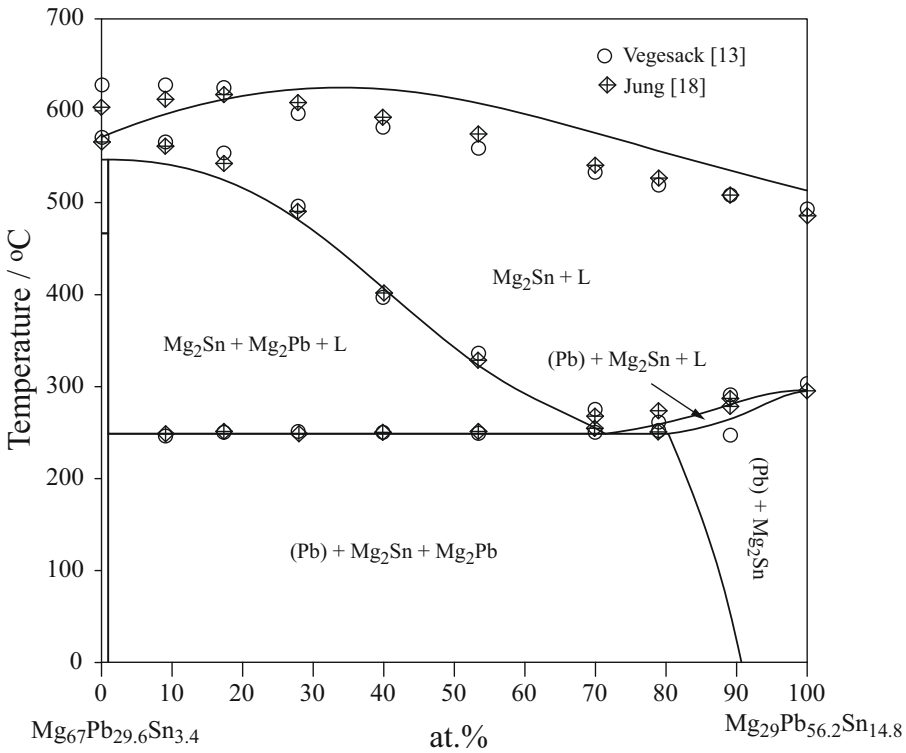

Fig. 13 The calculated vertical section of the $Mg_{67}Pb_{29.6}Sn_{3.4}$-$Mg_{29}Pb_{56.2}Sn_{14.8}$ section in the Mg-Pb-Sn system compared with experimental data of Vegesack[13, 18]

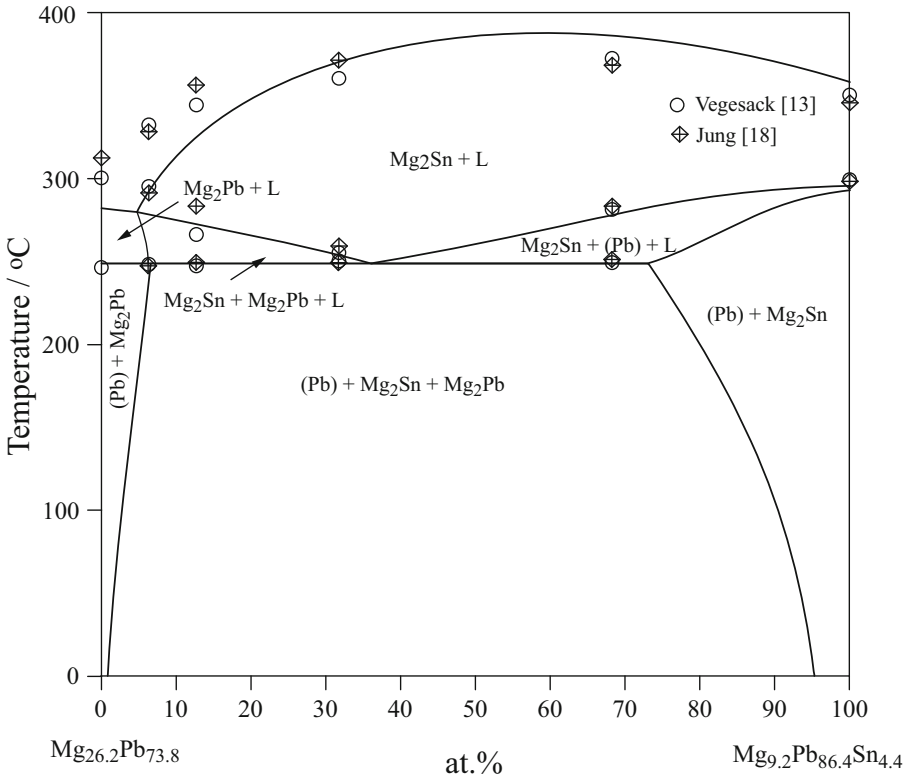

Fig. 14 The calculated vertical section of the $Mg_{26.2}Pb_{73.8}$-$Mg_{9.2}Pb_{86.4}Sn_{4.4}$ section in the Mg-Pb-Sn system compared with experimental data of Vegesack[13, 18]

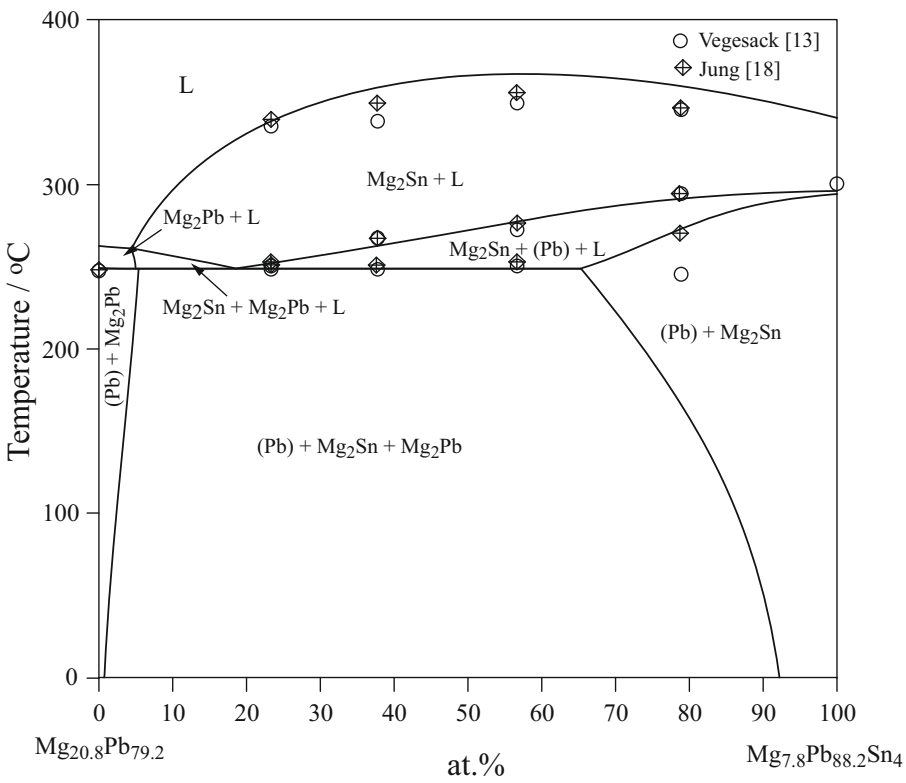

Fig. 15 The calculated vertical section of the $Mg_{20.8}Pb_{79.2}$-$Mg_{7.8}Pb_{88.2}Sn_4$ section in the Mg-Pb-Sn system compared with experimental data of Vegesack[13, 18]

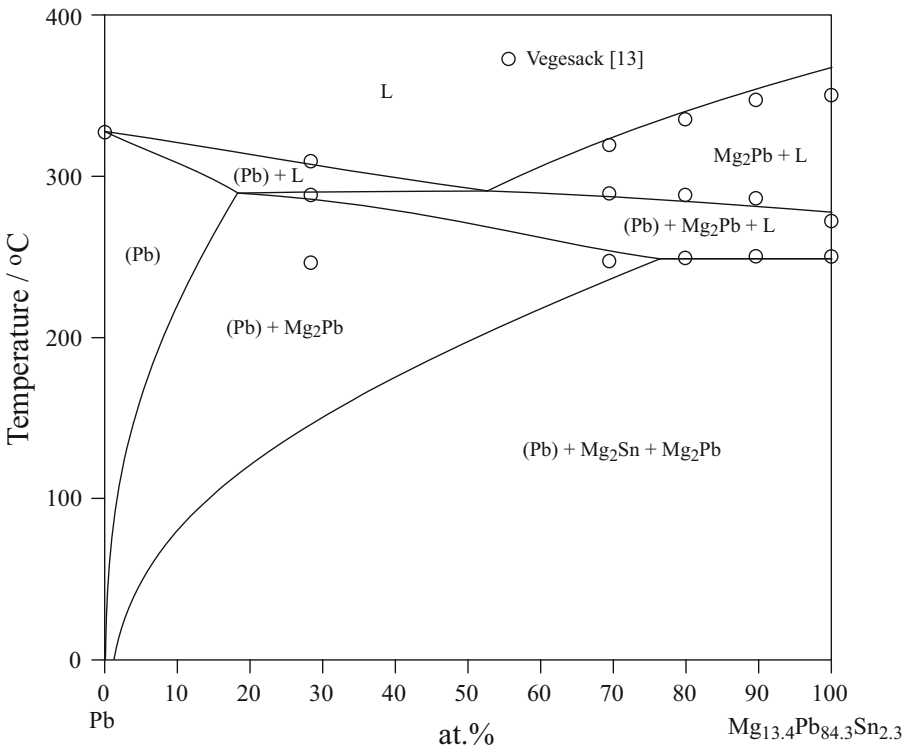

Fig. 16 The calculated vertical section of the Pb-$Mg_{13.4}Pb_{84.3}Sn_{2.3}$ section in the Mg-Pb-Sn system compared with experimental data of Vegesack[13]

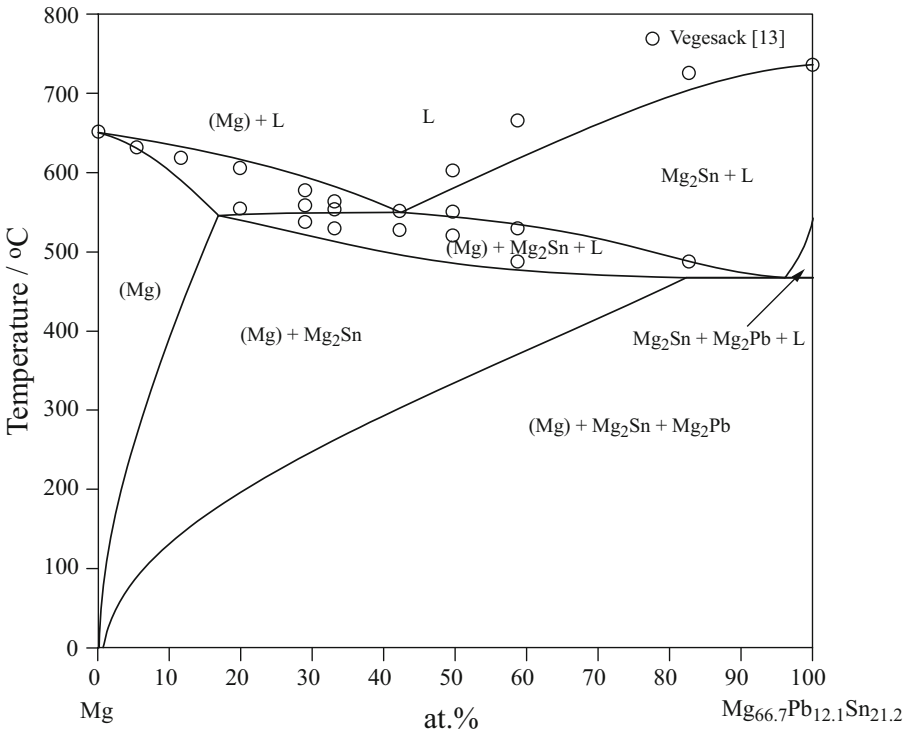

Fig. 17 The calculated vertical section of the Mg-$Mg_{66.7}Pb_{12.1}Sn_{21.2}$ section in the Mg-Pb-Sn system compared with experimental data of Vegesack[13]

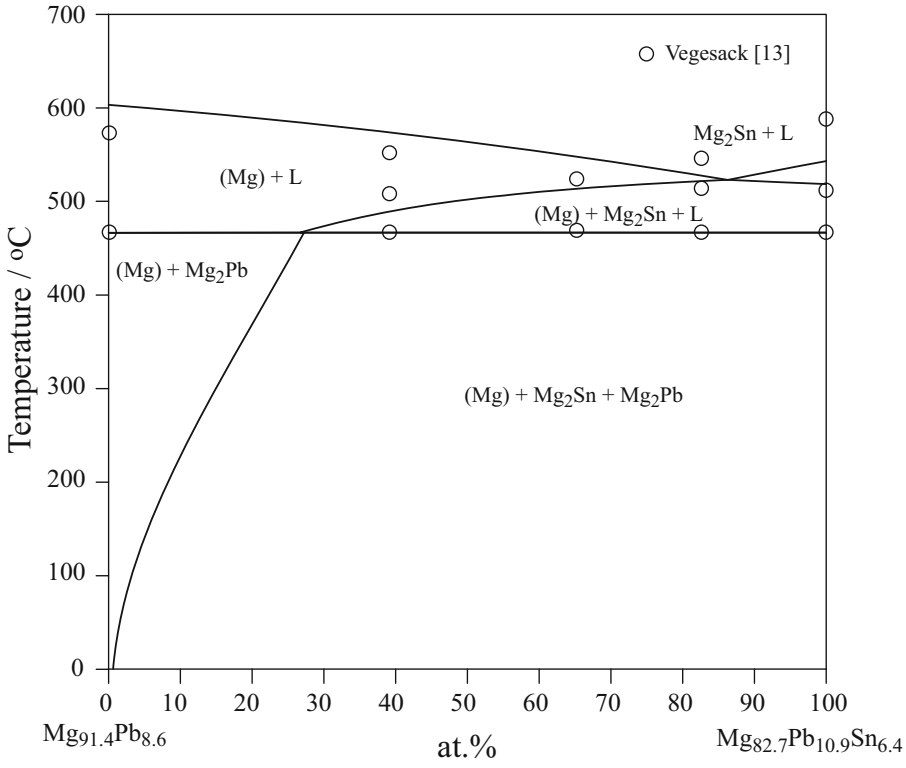

Fig. 18 The calculated vertical section of the $Mg_{91.4}Pb_{8.6}$-$Mg_{82.7}Pb_{10.9}Sn_{6.4}$ section in the Mg-Pb-Sn system compared with experimental data of Vegesack[13]

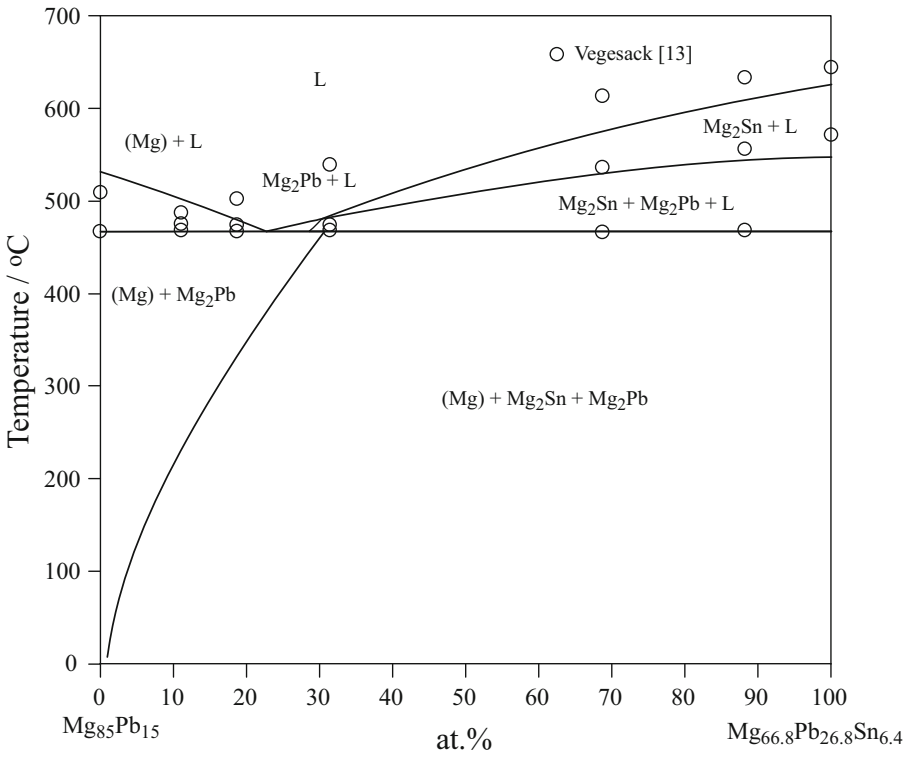

Fig. 19 The calculated vertical section of the $Mg_{85}Pb_{15}$-$Mg_{66.8}Pb_{26.8}Sn_{6.4}$ section in the Mg-Pb-Sn system compared with experimental data of Vegesack[13]

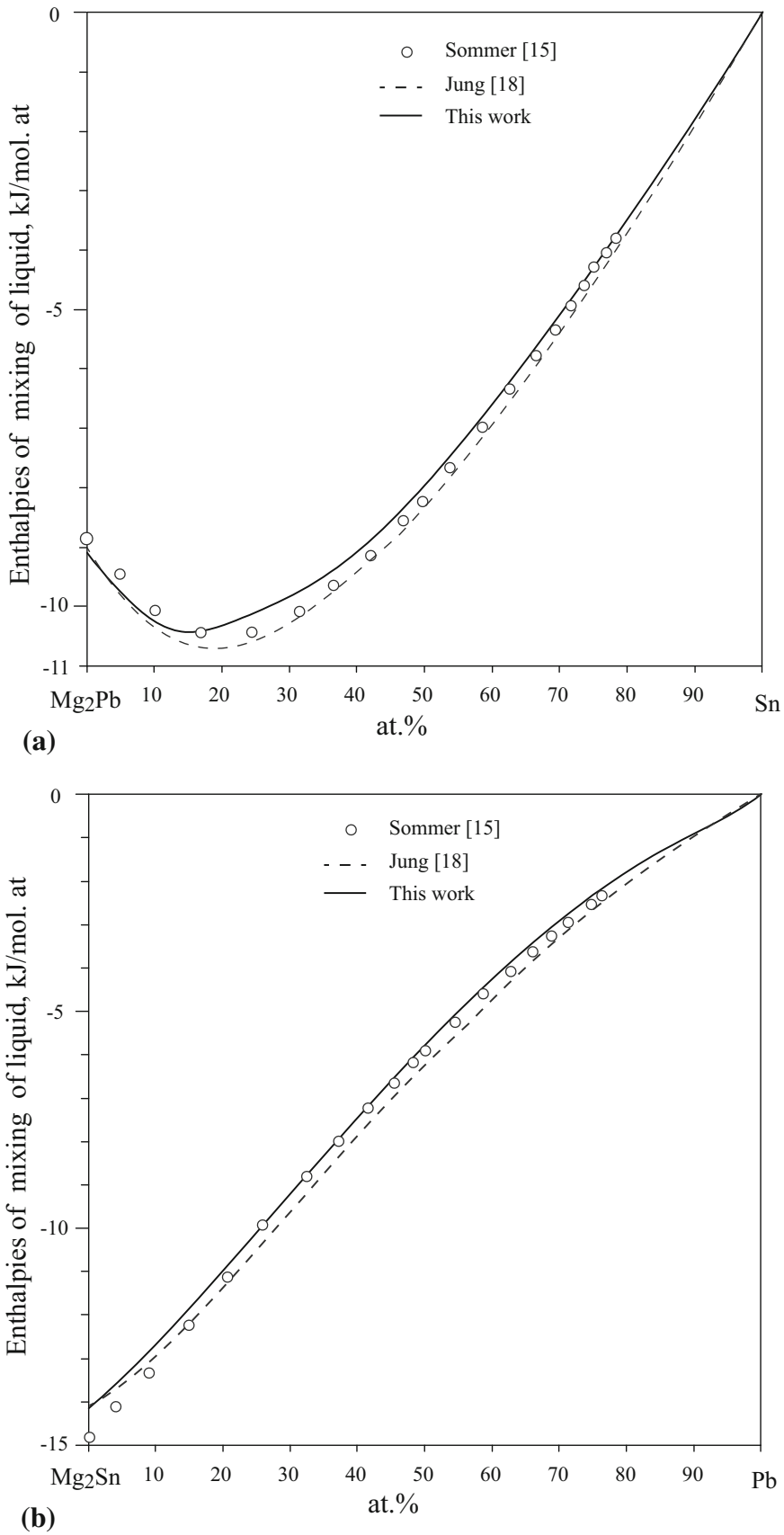

Fig. 20 The calculated enthalpies of mixing of liquid: (a) Mg_2Pb-Sn; (b) Mg_2Sn-Pb at 835 °C compared with the literature data[15, 18]

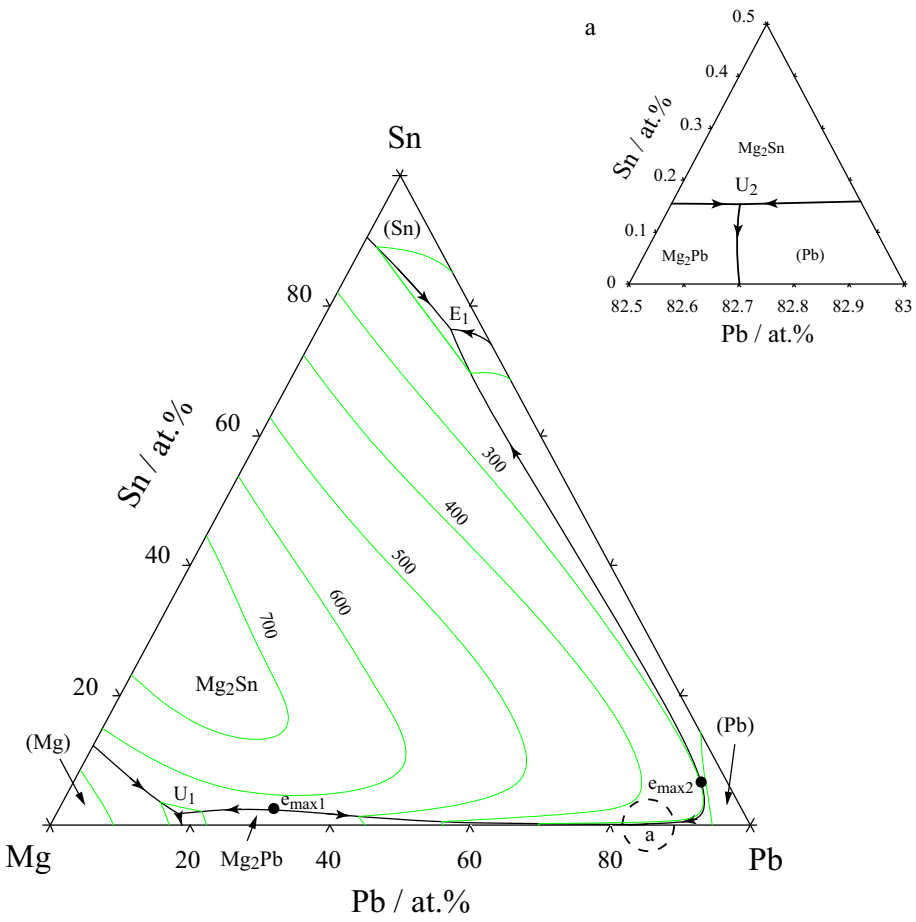

Fig. 21 The calculated liquidus projection of the Mg-Pb-Sn ternary system in the present work

interaction parameters in the Mg-Pb-Sn ternary system, and is expressed as follows:

$$^{m}L_{Mg:Pb,Sn} = a + bT, \qquad \text{(Eq 4)}$$

where the a and b were evaluated in the present work.

3.2 Calculated Results

In the Mg-Pb-Sn ternary system, all phase diagrams of the three sub-binary systems[26–28] have been thermodynamically assessed in the previous literatures. In the present work, the thermodynamic parameters of the three binary systems were directly adopted from the previous assessments. The thermodynamic parameters of each phase in the Mg-Pb-Sn system were optimized by both "manual" trial and error approach and PARROT[29] procedure. For the PARROT module in the THERMO-CALC[30] software, the literature data were used as input to the program. Each piece of selected information was given a certain weight by the importance of data, which reflected in many points, e.g. experimental error, equipment precision and knowledge development in the decade years etc. In the present research, the thermodynamic parameters were optimized the basis of the present experimental data and the previous work.[13, 15, 18] The parameters are changed by trial and error during the assessment, until most of the selected data are reproduced within the expected uncertainty limits. In the present work, all the mentioned literature data are used in the optimization process. All the parameters are eventually optimized to obtain the best consistency between the calculated results and literature data. All the optimized thermodynamic parameters of each phase in the Mg-Pb-Sn system are listed in Table 3, respectively.

The calculated isothermal sections of Mg-Pb-Sn ternary system at 200, 300 and 400 °C, compared with the experimental results determined in the present work, are presented in Fig. 4(a)-(c), respectively. The calculated results are in good agreement with most of the experimental data marked by different symbols. As seen in Fig. 4(a), there are four three-phase regions ((Mg) + Mg_2Pb + Mg_2Sn, Mg_2Pb + Mg_2Sn + (Pb), Mg_2Sn + (Pb) + Liquid, Mg_2Sn + (Sn) + Liquid). Two three-phase regions ((Mg) + Mg_2Pb + Mg_2Sn, Mg_2Pb + Mg_2Sn + Liquid) exist in the isothermal section at 300 °C (Fig. 4(b)). There are two three-phase regions ((Mg) + Mg_2Pb + Mg_2Sn, Mg_2Pb + Mg_2Sn + Liquid)

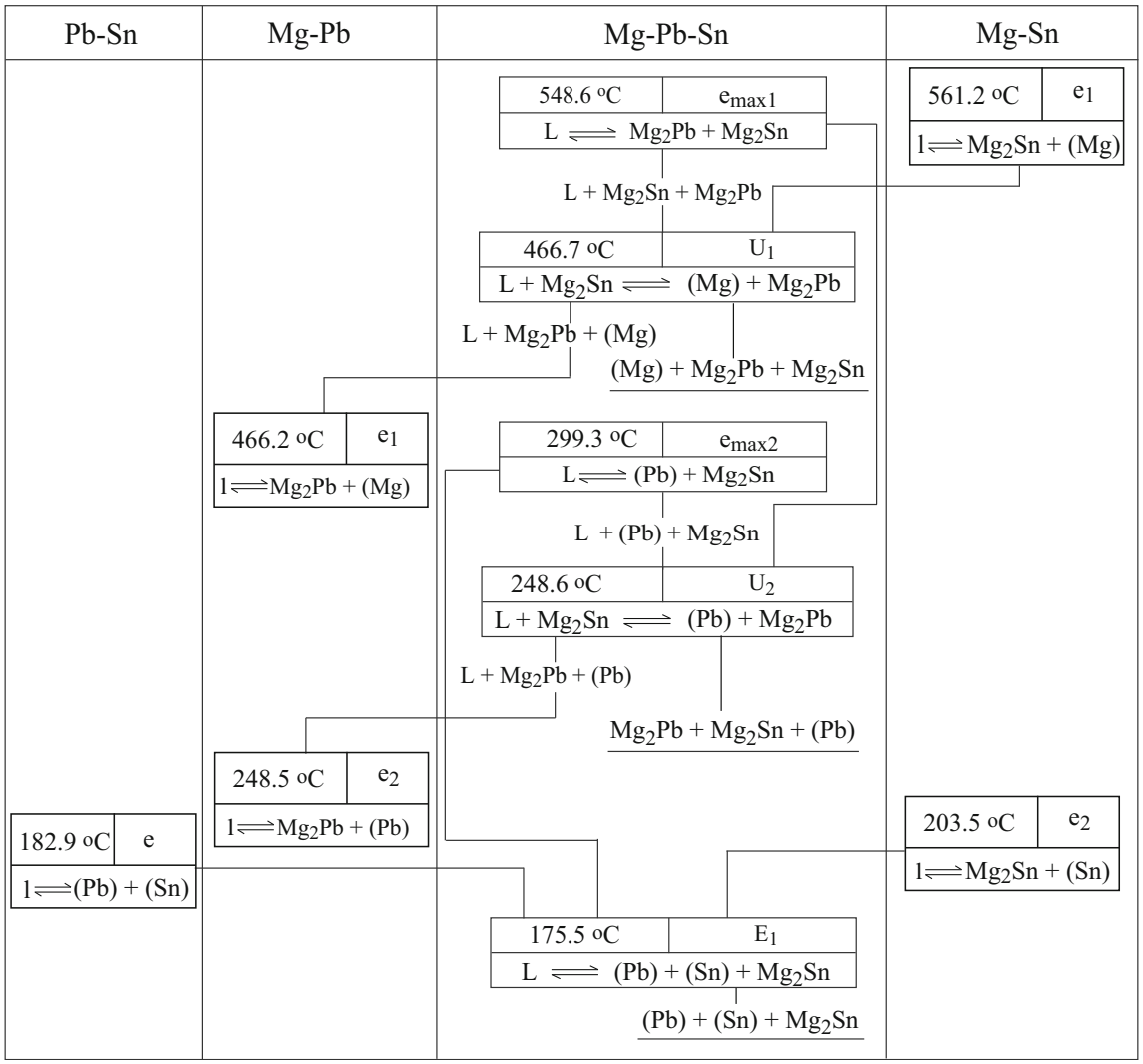

Fig. 22 The reaction scheme of invariant reactions in the Mg-Pb-Sn system

at 400 °C, as shown in Fig. 4(c). Mg_2Pb and Mg_2Sn were separated by a miscibility gap in our isothermal sections of Mg-Pb-Sn ternary system at 200, 300 and 400 °C. The results of calculated phase diagram were based on experimental data. The binary compounds are modeled as one intermetallic solution phase $Mg_2(Pb,Sn)_1$ because they share the same crystal structure. In the diagrams the Pb-rich $Mg_2(Pb,Sn)_1$ is denoted as "Mg_2Pb" and the Sn-rich $Mg_2(Pb,Sn)_1$ as Mg_2Sn". Therefore, the Mg_2Pb + Mg_2Sn two-phase region is in fact a miscibility gap.

The calculated vertical sections of the Mg-Pb-Sn ternary system with the experimental data[13, 17, 18] containing present work are presented in Fig. 5-19, respectively. The calculated vertical sections agree well with the experimental data,[13] while some figures show the acceptable deviation. The present calculated vertical section of the Mg_2Sn-Pb (as seen in Fig. 10) at low temperature shows major distinction with the results of Vegesack, Jung and Kim.[13, 18] The liquidus experimental data of Vegesack[13] are adequately considerated in the research process by Lukas,[17] while other experimental data are not selected. According to the present results of the isothermal section at 200 °C, the small region of the Mg_2Sn + Pb agrees well with the calculated result of the Lukas.[17] Therefore, the calculated Mg_2Sn-Pb section by Jung and Kim[18] at low temperature deviates unreasonably from the calculated results by Lukas[17] and the present calculated results. The calculated vertical sections of $Mg_{67}Pb_{29.6}Sn_{3.4}$-$Mg_{29}Pb_{56.2}Sn_{14.8}$ and $Mg_{26.2}Pb_{73.8}$-$Mg_{9.2}Pb_{86.4}Sn_{4.4}$ in Fig. 13 and 14 show a slight deviation from the experimental data.[13, 18] This deviation near the $Mg_{67}Pb_{29.6}Sn_{3.4}$ and $Mg_{26.2}Pb_{73.8}$ sides may result from the calculated results of Mg-Pb system.[26] Considering the consistency between the most of calculated results and experimental data,[13] we account that the optimized thermodynamic parameters in the present work are reasonable.

Table 4 The calculated invariant reactions in the Mg–Pb-Sn system compared with literature data[13, 17, 18]

Reaction	Type	Temperature/ °C	Composition		References
			at.% Pb	at.% Sn	
$L + Mg_2Sn \leftrightarrow Mg_2Pb$	p_1	548.6	31.9	2.1	This work
		555	32.3	1.0	Ref. 13
		555	32.3	1.0	Ref. 17
$L \leftrightarrow Mg_2Sn + (Pb)$	e_1	299.3	90.5	5.3	This work
		294	89.7	4.2	Ref. 13
		294	89.7	4.2	Ref. 17
$L + Mg_2Sn \leftrightarrow (Mg) + Mg_2Pb$	U_1	466.7	17.4	1.8	This work
		468	18.6	0.8	Ref. 13
		468	18.6	0.8	Ref. 17
		477.1	17.2	1	Ref. 18
$L + Mg_2Sn \leftrightarrow (Pb) + Mg_2Pb$	U_2	248.6	82.6	0.2	This work
		250	83	0.2	Ref. 13
$L \leftrightarrow (Pb) + Mg_2Pb + Mg_2Sn$	D_1	249	83	0.2	Ref. 17
		254.3	83.8	0.1	Ref. 18
$L \leftrightarrow (Sn) + (Pb) + Mg_2Pb$	E_1	175.5	18.9	76.4	This work
		166	20.5	74.3	Ref. 13
		169	20.2	74.3	Ref. 17
		170.5	20.4	74.5	Ref. 18

The calculated enthalpies of mixing of liquid Mg-Pb-Sn alloys are compared with the experimental data[15] and the assessed results by Jung and Kim,[18] as shown in Fig. 20. The mixing enthalpies calculated from thermodynamic parameters are in agreement with the literature data.[15, 18] Figure 21 shows the calculated liquid projection of the Mg-Pb-Sn ternary system. The reaction scheme of the invariant reactions in the Mg-Pb-Sn ternary system is given in Fig. 22. The corresponding temperatures and compositions of the invariant reactions compared with literature data[13, 18] are given in Table 4. As can be seen, the calculated results including liquidus, solidus, temperatures and compositions of invariant reactions are in good agreement with most of the experimental data and the assessed result.[13, 15, 18]

4 Conclusions

Three isothermal sections of Mg-Pb-Sn ternary system at 200, 300 and 400 °C were experimentally determined. Based on the available literature data including the present phase equilibria and the previous thermodynamic properties, the thermodynamic asessments of the Mg-Pb-Sn ternary system have been carried out by using the CALPHAD technique. A consistent set of optimized thermodynamic parameters has been derived for describing the Gibbs free energy of each phase in the Mg-Pb-Sn ternary system, while a good agreement between the calculated results and most of the experimental data has been obtained.

Acknowledgments This work was financially supported by the Science and Technology Bureau of Xiamen City (Project No. 3502Z20131153). This work was supported by the National Natural Science Foundation of China (Grant No. 51171159) and the Ministry of Education of China (Grant No. 20120121130004). The support from the Ministry of Science and Technology of China (Grant No. 2012CB825700 and 2014DFA53040) is also acknowledged.

References

1. R.F. Koontz and R.D. Lucero, Magnesium Water-Activated Batteries, *Handb. Batter.*, 2002, **17**(1-17), p 27
2. J. Zhao, K. Yu, Y.N. Hu, S.J. Li, X. Tan, F.W. Chen, and Z.M. Yu, Discharge Behavior of Mg-4 wt%Ga-2 wt%Hg Alloy as Anode for Seawater Activated Battery, *Electrochim. Acta*, 2011, **56**, p 8224-8231
3. M.G. Medeiros and E.G. Dow, Magnesium-Solution Phase Catholyte Seawater Electrochemical System, *J. Power Sources*, 1999, **80**, p 78-82
4. D.X. Cao, L. Wu, Y. Sun, G.L. Wang, and Y.Z. Lv, Electrochemical Behavior of Mg-Li, Mg-Li-Al and Mg-Li-Al-Ce in Sodium Chloride Solution, *J. Power Sources*, 2008, **177**, p 624-630
5. L. Yu and X.G. Zhang, Electrochemical Insertion of Magnesium Ions into V2O5 from Aprotic Electrolytes with Varied Water Content, *J. Colloid Interface Sci.*, 2004, **278**, p 160-165
6. M.C. Lin, C.Y. Tsai, and J.Y. Uan, Electrochemical Behaviour and Corrosion Performance of Mg-Li-Al-Zn Anodes with High Al Composition, *Corros. Sci.*, 2009, **51**, p 2463-2472
7. D. Wang, Y. Yu, X. Liu, and C. Wang, Thermodynamic Assessment of the Eu-Pb and Lu-Pb Systems, *Calphad*, 2013, **41**, p 20-25

8. D.X. Cao, L. Wu, G.L. Wang, and Y.Z. Lu, Electrochemical oxidation behavior of Mg-Li-Al-Ce-Zn and Mg-Li-Al-Ce-Zn-Mn in sodium chloride solution, *J. Power Sources*, 2008, **183**, p 799-804
9. Y.Z. Lv, M. Liu, Y. Xu, D.X. Cao, and F. Jing, The Electrochemical Behaviors of Mg-8Li-3Al-0.5 Zn and Mg-8Li-3Al-1.0 Zn in Sodium Chloride Solution, *J. Power Sources*, 2013, **225**, p 124-128
10. Y. Feng, R.C. Wang, K. Yu, C.Q. Peng, J.P. Zhang, and C. Zhang, Activation of Mg–Hg Anodes by Ga in NaCl Solution, *J. Alloys Compd.*, 2009, **473**, p 215-219
11. S. Khireche, D. Boughrara, A. Kadri, L. Hamadou, and N. Benbrahim, Corrosion Mechanism of Al, Al-Zn and Al-Zn-Sn Alloys in 3 wt% NaCl Solution, *Corros. Sci.*, 2014, **87**, p 504-516
12. R. Udhayan, N. Muniyandi, and P.B. Mathur, Studies on magnesium and its alloys in battery electrolytes, *Br. Corros. J.*, 1992, **27**, p 68
13. A. Vegesack, Uber die ternaren Legierungen von Blei, Magnesium und Zinn, *Z. Anorg. Chem.*, 1907, **54**, p 376-416
14. S.A. Pogodin and L.M. Kefeli, Investigation of Mg-rich Ternary Solid Solutions in the Mg-Pb-Sn System, *Izv. Sekt. Fiz.-Khim. Anal.*, 1949, **18**, p 86-91
15. F. Sommer, N. Rupf-Bolz, and B. Predel, Investigations on the Temperature Dependence of the Mixing Enthalpy of Ternary Alloy Melts, *Z. Metallkd.*, 1983, **74**, p 165-171
16. W.J. Howell and C.A. Eckert, A Linear Chemical-Physical Theory Model for Ternary Liquid Metal Solutions, *Z. Metallkd.*, 1990, **81**, p 335-340
17. H.L. Lukas, Magnesium-Lead-Tin. MSI Eureka, 2001
18. I.H. Jung and J. Kim, Thermodynamic Modeling of the Mg-Ge-Si, Mg-Ge-Sn, Mg-Pb-Si and Mg-Pb-Sn systems, *J. Alloys Compd.*, 2010, **494**, p 137-147
19. L. Kaufman and H. Bernstein, *Computer Calculation of Phase Diagram*, Academic Press, New York, 1970
20. N. Saunders and A.P. Miodownik, *CALPHAD-A Comprehensive Guide*, Pergamon Press, Oxford, 1998
21. H.L. Lukas, S.G. Fries, and B. Sundman, *Computational Thermodynamics-The Calphad Method*, Cambridge University Press, Cambridge, 2007
22. A.A. Nayeb-Hashemi and J.B. Clark, The Mg-Pb (Magnesium-Lead) System, *Bull. Alloy Phase Diagr.*, 1985, **6**, p 56-66
23. A.A. Nayeb-Hashemi and J.B. Clark, The Mg-Sn (Magnesium-Tin) system, *Bull. Alloy Phase Diagr.*, 1984, **5**, p 466-476
24. I. Karakaya and W. Thompson, The Pb-Sn (Lead-Tin) system, *J. Phase Equilibria.*, 1988, **9**, p 144-152
25. O. Redlich and A.T. Kister, Thermodynamics of nonelectrolyte solutions-x-y-t relations in a binary system, *Ind. Eng. Chem.*, 1948, **40**, p 341-345
26. D. Wang, S.Y. Yang, X.J. Liu, J.G. Duh, and C.P. Wang, Experimental investigation and thermodynamic calculation of phase equilibria in the Mg-Pb-Zn ternary system, *Mater. Chem. Phys.*, 2016, **171**, p 227-238
27. F.G. Meng, J. Wang, L.B. Liu, and Z.P. Jin, Thermodynamic modeling of the Mg-Sn-Zn ternary system, *J. Alloy. Compd.*, 2010, **508**, p 570-581
28. H. Ohtani, K. Okuda, and K. Ishida, Thermodynamic Study of Phase Equilibria in the Pb-Sn-Sb System, *J. Phase Equilibria.*, 1995, **16**, p 416-429
29. B. Jansson, Thesis, Royal Institute of Technology, Staockolm, 1983
30. J.O. Andersson, T. Helander, L. Höglund, P.F. Shi, and B. Sundman, Thermo-Calc & DICTRA, Computational Tools for Materials Science, *CALPHAD*, 2002, **26**, p 273-312